



# Texture Evolution of Hard-Templated Hierarchically Porous Alumina Catalyst in Heavy Oil Hydroprocessing

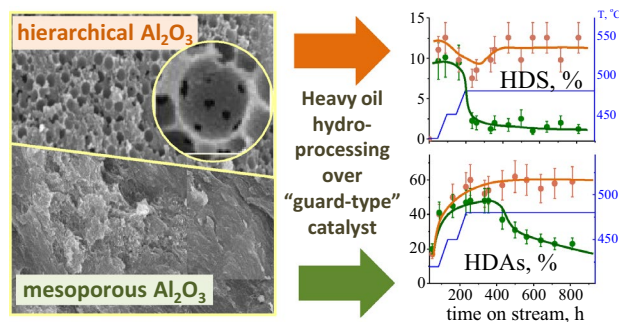
Viktoriya S. Semeykina<sup>1</sup> · Alexander V. Polukhin<sup>1</sup> · Anton I. Lysikov<sup>1</sup> · Andrey V. Kleymentov<sup>2</sup> · Konstantin V. Fedotov<sup>2</sup> · Ekaterina V. Parkhomchuk<sup>1</sup>

Received: 16 August 2018 / Accepted: 18 December 2018 / Published online: 7 January 2019  
© Springer Science+Business Media, LLC, part of Springer Nature 2019

## Abstract

The study is devoted to the deactivation behavior of alumina “guard-type” mesoporous and hierarchical catalysts in long-term 800 h hydroprocessing of heavy oil under conditions close to industrial ones. The purely mesoporous sample had only 10–15 nm mesopores by Hg porosimetry whereas the hierarchical catalyst possessed a bimodal pore size distribution with maximum at 15 nm (55 vol%) and 40 nm (45 vol%, related to the mouths of 200 nm spherical macropores). Both catalysts had similar activities for the first 200 h of hydroprocessing. The mesoporous catalyst underwent the rapid deactivation in hydrodesulfurization (HDS) and hydrodemetallization (HDM) of V after 200 h on stream, and the remarkable decrease in hydrodeasphaltenization (HDAs) and Ni removal after 300–400 h on stream due to the intensive mesopore plugging by 55% of the total volume. The hierarchical catalyst did not show any decline in HDS and HDAs during the 800 h experiment, though its HDM activity also reduced due to the surface poisoning and coke deposition, albeit to a lesser extent. The intrinsic mesopores of the hierarchical alumina were shown to narrow down to 10 nm but did not experience substantial blocking observed for the mesoporous catalyst. Hierarchical texture seems not only to provide wide macro- and mesopores less prone to plugging by coke species, but to ensure effective transport of reaction products out of the small pores which prevents them from blockage.

## Graphical Abstract



**Keywords** Heavy oil · Hydroprocessing · Deactivation · Hierarchical · Heterogeneous catalysis · Texture

**Electronic supplementary material** The online version of this article (<https://doi.org/10.1007/s10562-018-2646-3>) contains supplementary material, which is available to authorized users.

✉ Viktoriya S. Semeykina  
viktoriyacatalysis@gmail.com

Extended author information available on the last page of the article

## 1 Introduction

Despite a rapid development of alternative energetics, heavy oils and residues still represent a considerable fraction among other energy sources, especially in regard to producing liquid fuels and lubricants [1]. Catalytic hydroprocessing of heavy hydrocarbons in a fixed bed reactor is

the most widely spread approach frequently used in combination with more sophisticated technologies (moving-bed, ebullated-bed, slurry reactor) [2–4].

The key problem of this approach consists in rapid catalyst deactivation caused by deposition of carbon and metal abundant in heavy feeds. These species are known not only to cover catalytically active sites, but, more importantly, to block small mesopores which results in dramatic decrease of available surface area [4, 5]. To reduce diffusional limitations and delay complete plugging of the porous structure, catalysts with wider pore size and higher pore volume are needed.

According to a set of theoretical and experimental studies on the initial catalytic activity, the mesopore size in the range of 10–35 nm is sufficient for lowering diffusional restrictions in hydrodesulfurization (HDS), hydrodemetallization (HDM) and hydrodeaspaltenization (HDAs) of heavy feed, with the optimal pore size for HDM and HDAs usually being larger than that for HDS [6–11]. However, when it comes to a large amount of coke and metal deposits, the abovementioned mesopores are not able to effectively prevent the pores from gradual narrowing and blocking [12]. S. M. Rao and M.-O. Coppens in their theoretical study showed that the catalyst with a hierarchical texture containing 30% of ~200 nm macropores and 70% of ~30 nm mesopores is more preferable over the sample with the purely mesoporous texture (~30 nm mesopores) in terms of lifetime, despite the lower initial catalytic activity [13]. The idea of using the hierarchical texture was also embodied in some experimental studies, which pointed out the importance of large (~100 nm) macropores in transformation of high molecular weight reagents [12, 14–18].

Approaches for preparation of the supports with hierarchical texture are numerous and could conventionally be divided into template-free methods and techniques involving templates. In the template-free methods, the formation of hierarchical porosity could be driven by spinodal decomposition [19, 20] or hydrothermal recrystallization, which are often controlled by various additives. Among these methods especially interesting for industry are the hydrothermal treatment of alumina with the formation of ~100 nm pores [21], the hydrothermal synthesis of alumina from  $\text{Al}_2(\text{SO}_4)_3$  without additives [15] or using poly-glycol [22], citric acid [14] and methenamine [23], the hydrothermal synthesis of “urchin-like” alumina [24].

To produce supports with a tunable macro- and mesoporous structure, a template method is widely employed since it is rather simple and quite universal in relation to the choice of precursor. So called “soft” templates are usually suitable for creation of large mesopores (non-ionic surfactants [25, 26], starch, gelatin, dextrin and sugar [27, 28]), and “hard” templates are more preferable

for formation of macropores (soot [29], oil residua [30], sawdust [28], cellulose [31], polymers [32–36]).

Among all the techniques mentioned, the “hard” template method using monodisperse 200 nm polymer microspheres was chosen since it enabled a thorough control over the fraction, size and shape of macropores to study the effect of hierarchical porosity on catalyst deactivation. A simple and low-cost synthesis makes polymer microspheres a perspective additive for preparation of hierarchical supports in a large scale as well.

Previously, we have carried out some theoretical estimations showing that hierarchical texture remained permeable after almost complete mesopore blocking, which seemed to be the main factor for prolongation of catalyst lifetime [37]. Here we show in details the experimental data on the deactivation behavior of the mesoporous and hierarchically porous “guard-type” catalysts in heavy oil hydroprocessing under the conditions close to industrial ones. The catalysts were studied without the addition of the active component  $\text{Co}(\text{Ni})\text{Mo}(\text{W})\text{S}$  to ensure that the effects observed were related only to the textural differences.

## 2 Experimental Section

### 2.1 Materials

The following chemicals were used: stabilized styrene (pure grade, Angara reaktiv), sodium hydroxide NaOH (analytical grade, Reakhim), 4,4'-azobis(4-cyanovaleric acid) (>98%, Aldrich), pseudoboehmite  $\text{AlOOH}\cdot\text{H}_2\text{O}$  (Promyshlennye katalizatory), nitric acid  $\text{HNO}_3$  (reagent grade, Reakhim), poly(ethylene glycol)-block-poly(propylene glycol)-block-poly(ethylene glycol) (Aldrich,  $M_w = 5800$ ) and distilled  $\text{H}_2\text{O}$ .

Heavy oil from Tatar republic has been chosen as a heavy feedstock for hydroprocessing experiments. The feed had high S content (4.3 wt%), moderate metal content (200 ppm V, 60 ppm Ni), high viscosity (3710 sSt) and density ( $0.960 \text{ g/cm}^3$ ) at 25 °C. The chemical composition of the feed was represented by 25.4 wt% of saturates, 44.7 wt% of aromatics, 23.7 wt% of resins and 6.4 wt% of asphaltenes (the estimated size of  $2.7 \pm 0.1 \text{ nm}$  at ambient conditions [38]). The fractional composition of the feed was the following: 1.9 wt% gasoline (0–180 °C), 21.6 wt% of diesel (180–360 °C), 33.5 wt% of atmospheric gasoil (360–550 °C), 14.8 wt% of vacuum gasoil (550–720 °C) and 28.4 wt% of residue (>720 °C). For more detailed information on the properties of the feed see Supplementary materials Table 1S.

## 2.2 Catalyst Preparation

A suspension of polystyrene (PS) microspheres (5 wt%, 250 nm, carboxylic surface groups), used as a template for the preparation of the hierarchical alumina, was synthesized by emulsion polymerization under conditions similar to that described elsewhere [39]. For the preparation of the hierarchical “guard-type” catalyst, the suspension was mixed with  $\text{AlOOH}\cdot\text{H}_2\text{O}$  powder to produce a precipitate containing 20 wt% of the template. The precipitate was dried at room temperature and grounded to the particles less than 0.45 mm in size. A solution comprising 0.033 g of  $\text{HNO}_3$  and 0.033 g of block-copolymer per gram of  $\text{Al}_2\text{O}_3$  was added to the mixture in a quantity sufficient to produce a paste. The paste was kneaded for 30 min and then extruded into cylindrical pellets ( $3\times 5$  mm), dried in air for 1 day and heat treated in air for 4 h at 800 °C with a heating rate of 100 °C  $\text{h}^{-1}$ . The sample obtained was referred to as  $\text{Al}_2\text{O}_3\text{-T}$ . The reference alumina with purely mesoporous texture, designated as  $\text{Al}_2\text{O}_3$ , was prepared by the same technique without the PS template.

## 2.3 Catalyst Characterization

Before physico-chemical characterization, the spent catalysts were subjected to extraction by toluene in a Soxhlet’s apparatus for 48 h to remove reaction products. The fresh catalysts were investigated without additional pretreatments.

Isotherms of  $\text{N}_2$  adsorption/desorption at 77 K ( $\text{N}_2/77$  K) were measured after degassing the samples in a vacuum of 6 mTorr at 200 °C for 4 h with an Autosorb-6B-Kr instrument (Quantachrome Instruments, USA). Mercury porosimetry was carried out on an AutoPore IV 9500 porosimeter (Micromeritics). Pycnometric density of the catalysts was determined on an automatic density analyzer Ultrapyc 1200e (Quantachrome Instruments, USA). Scanning electron microscopy (SEM) images were taken with a JSM\_6460LV microscope at an accelerating voltage of 15–20 kV. Phase composition was studied with X-ray diffraction recorded on a Bruker D8 Advanced diffractometer (2011, Germany) using  $\text{CuK}\alpha$  monochromatic radiation ( $\lambda = 1.5418$  Å) with a step of  $2\theta = 0.05^\circ$  and a storage time of 1–2 s.

Study of the acidic properties of the catalysts was carried out by thermo programmed  $\text{NH}_3$  desorption (TPD- $\text{NH}_3$ ) using a quadrupole mass spectrometer HiCube RGA100. Temperature was controlled using a Termodat 13KT2/5T supplying a continuous heat rate of the sample. Crushing strength of the fresh catalysts was estimated by measuring a breaking force for a pellet compressed between two parallel plates using a MP-9S testing machine. An average value was found using statistical data on 30 pellets. Thermogravimetric analysis (TGA) and differential thermal analysis (DTA) were carried out on a Q1500

D derivatograph (MOM) at a heating rate of 10°C/min, a flow rate of 50 ml/min in air atmosphere.

Elemental composition of the catalysts was determined by X-ray fluorescent spectroscopy with synchrotron radiation (SR XFS) in a storage ring VEPP-3, Siberian Synchrotron and Terahertz Radiation Center (Budker Institute of Nuclear Physics SB RAS, Novosibirsk, Russia). The parameters of VEPP-3 were as follows:  $E_{\text{ex}} = 2$  GeV,  $B = 2\text{T}$ , and  $I_e = 100$  mA.

## 2.4 Catalytic Experiments and Product Characterization

Heavy oil hydrotreating experiments were carried out using a lab scale Berty reactor as described in the previous paper [40]. The same volume of catalyst pellets was loaded into the reactor to compare performance of the catalysts with different texture. Hydroprocessing parameters were as follows: pressure 7 MPa, feed to  $\text{H}_2$  volume ratio 1000, liquid hourly space velocity LHSV 1.0  $\text{h}^{-1}$ , time on stream 800 h. The temperature of the process was increased from 420 to 480 °C during the first 200 h of the experiment to enhance thermal cracking and achieve better activity in removal of asphaltenes and impurities (S, V, Ni). There must be significant intraparticle and low-to-moderate interparticle diffusion limitations in the systems studied, just as in a typical industrial process, but no temperature gradients (see Supplementary Material).

Sulfur content in the hydrotreated products was determined by a X-ray fluorescence analyzer HORIBA SLFA 2100 (Japan) in accordance with the protocol GOST R 50442-92 with a relative error of 0.1%. Elemental composition of the oil products was studied by SR XRF analysis. Density and viscosity of the feed and oil products was measured with a SVM 3000 instrument (Anton Paar, USA) under the protocol ASTM D7042, fractional composition—by simulated distillation according to the protocol ASTM 7169.

Activity of the catalysts was estimated using HDS, HDAs or HDM conversion values

$$X = \frac{C_i^0 - C_i}{C_i^0} \cdot 100\%,$$

Where  $C_i^0$  and  $C_i$  are the initial and final concentrations of sulfur, asphaltene or metal (Ni + V) in the feed and oil products.

## 3 Results and Discussion

### 3.1 Properties of the Fresh Catalysts

Two “guard-type” catalysts used in this work for heavy oil hydroprocessing comprised of alumina pellets with purely

mesoporous or hierarchical texture. Since the catalytic experiments were carried out using similar volumes of the samples just as in a real process, all textural properties were recalculated per volume of the catalyst using a true density parameter. This normalization was especially reasonable with regard to the data on the spent catalysts because it relieved the necessity to allow for the contribution of coke and metal deposits to the catalyst weight.

The mesoporous texture of the hierarchical catalyst was less developed according to the specific values of BET surface area and mesopore volume. This fact could probably be explained by more intensive sintering of mesopores upon combustion of the template accompanied by local overheating and gas release (Table 1; Fig. 1).

The total pore volume of the hierarchical sample, on the contrary, exceeded that of the mesoporous catalyst due to the contribution of macropores, which is clearly seen in the integral pore size distribution (PSD) plot according to Hg porosimetry (Table 1; Fig. 1b).

The plot clearly demonstrates that the  $\text{Al}_2\text{O}_3$  sample had only mesopores 10–15 nm in size, whereas the hierarchical  $\text{Al}_2\text{O}_3\text{-T}$  shows a bimodal pore size distribution with maximum at 15 nm and 40 nm. The former are ascribed to the slightly sintered intrinsic mesopores of alumina, while the latter could be attributed to the mouths

of spherical macropores with the diameter of about 180–200 nm, observed in the SEM images (Fig. 2a). Apparently, spherical macropores cannot be filled with Hg at the appropriate pressure because of the “bottle-neck” effect, so this process occurs through narrow mouths, which is seen as an ascent at 40 nm in the PSD plot.

Phase composition of the samples was represented by a mixture of  $\gamma$ - and  $\delta$ - $\text{Al}_2\text{O}_3$  with the average crystallite size of 5.5–7.8 nm (see Supplementary Materials Fig. 1Sa). The concentration and strength of surface acidic groups seem to be similar for both catalysts according to TPD- $\text{NH}_3$ : approximately  $0.8 \mu\text{mol NH}_3/\text{m}^2$  was desorbed from the samples (see Supplementary Materials Fig. 1Sb). Since the difference in quantity of acidic sites and desorption temperatures lies within the error limit of the method, one can assume that both the catalysts, prepared from the same precursor and under the same mixing, drying and calcining conditions, have almost identical acidic surface properties.

### 3.2 Catalytic Experiments

The long-term experiments on heavy oil hydroprocessing demonstrated different dynamics of deactivation for the hierarchical and mesoporous “guard-type” catalyst. According to the analysis of the oil products, the mesoporous sample

**Table 1** Textural properties of the fresh and spent catalysts, normalized to mass and volume of pellets

Sample	Crushing strength Units	$\rho_{\text{true}}$ g/cm <sup>3</sup>	$S_{\text{BET}}$		$V_{\text{N}_2}$		$V_{\text{total}}$		$V_{\text{macro}}$ cm <sup>3</sup> /cm <sup>3</sup>
			m <sup>2</sup> /g	m <sup>2</sup> /cm <sup>3</sup>	cm <sup>3</sup> /g	cm <sup>3</sup> /cm <sup>3</sup>	cm <sup>3</sup> /g	cm <sup>3</sup> /cm <sup>3</sup>	
$\text{Al}_2\text{O}_3$	$4.5 \pm 1.0$	3.271	121	145	0.55	0.66	0.53	0.63	–
$\text{Al}_2\text{O}_3$ 800 h	–	2.213	65	105	0.19	0.31	0.17	0.27	–
$\text{Al}_2\text{O}_3\text{-T}$	$2.5 \pm 0.8$	3.312	100	90	0.37	0.33	0.81	0.73	0.32
$\text{Al}_2\text{O}_3\text{-T}$ 800 h	–	2.180	116	119	0.55	0.56	0.52	0.53	0.26

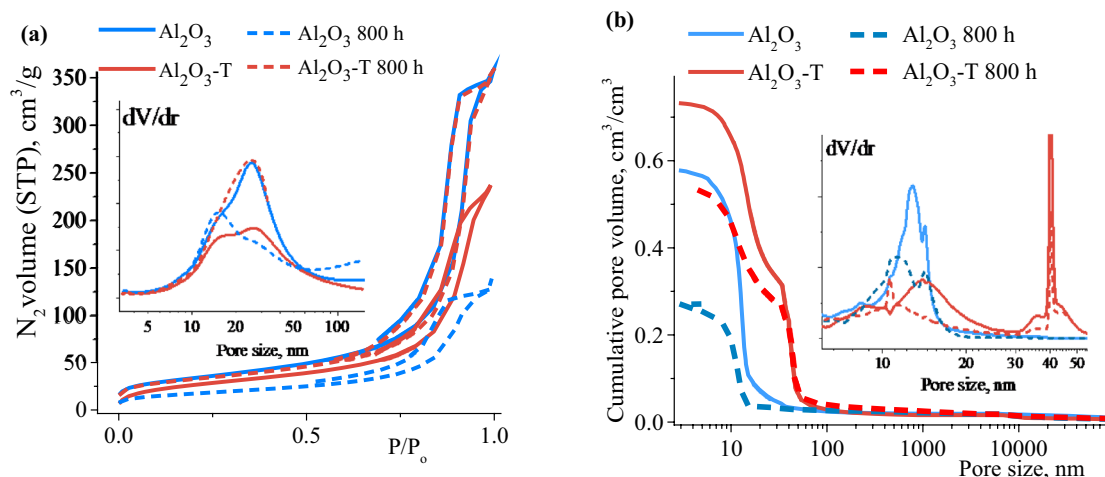


**Fig. 1** Textural properties of the fresh and spent catalysts: adsorption/desorption isotherms of  $\text{N}_2$  at 77 K and corresponding PSD (a) and integral/differential PSD according to Hg porosimetry (b)

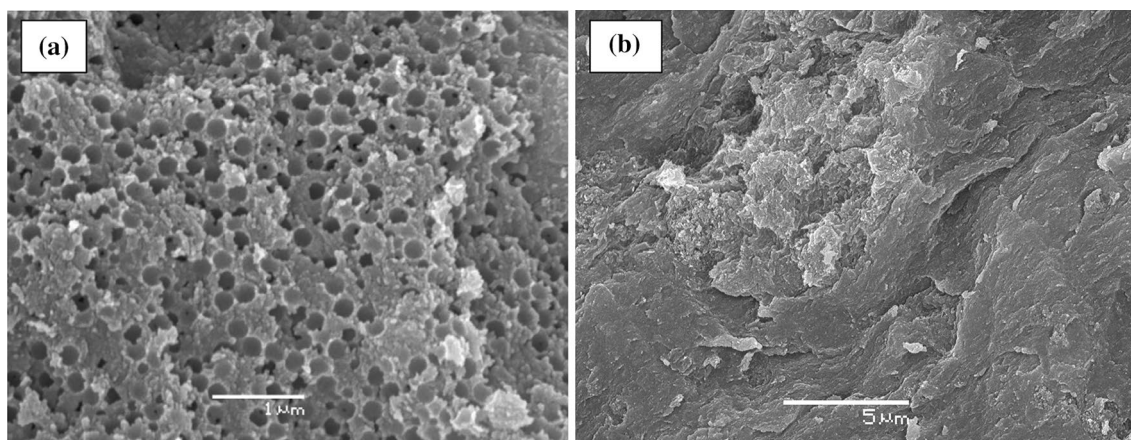


**Fig. 2** SEM images of the hierarchically porous (a) and mesoporous (b) alumina

experienced a rapid decrease in HDS after 200 h under hydroprocessing conditions (Fig. 3a). The conversion of asphaltenes for this catalyst significantly increased from 20 to 45% due to the rise of temperature for the first 200 h and underwent a permanent decline to the initial value after 400 h (Fig. 3b). A similar trend was also observed for HDM: the metal conversion increased up to 50–60% with temperature for the first 100 h but went down to less than 10% after 200 h for V and 400 h for Ni (Fig. 3c, d).

The initial activity of the hierarchical catalyst was similar to that of the mesoporous one: HDS showed a slight decrease, HDAs and HDM—a substantial increase with temperature for the first 200 h of hydroprocessing (Fig. 3). However, the experiments demonstrated that conversions of S-containing molecules and asphaltenes had no further decline and reached a plateau after 400 h until the end of the catalytic tests. A slight increase in S removal after 250 h could be ascribed to deposition of Ni and V sulfides, which possess some hydrogenation and cracking activity observed by other researchers [41, 42]. HDM of the hierarchical sample was found to fall down after 100 h on stream as well, albeit to a lesser extent in comparison with the mesoporous catalyst. Although metal content in oil products shows rather big data spread due to inhomogeneity of the probes and the effect of metal surrounding on the XF signal intensity, it is reasonable to assume that HDM of the hierarchical catalyst was higher throughout the whole experiment.

Calculation of the overall catalytic activities of the hierarchical sample, based on the properties of the “averaged” mixed product obtained during 800 h of experiment, gave the following values: HDS—12%, HDM V—26%, HDM Ni—32%, HDAs—57%. Since the alumina “guard-type” catalyst had moderate acidic surface groups and no active NiMoS phase, it was able to provide only moderate cracking of large hydrocarbons. It contributes to a small increase in gasoline fraction (+0.6 wt%), a notable increase in diesel

(+5.1 wt%) and atmospheric gasoil (+1.6 wt%) and reduce in vacuum gasoil (−0.9 wt%) and residue fraction (−6.4 wt%). All in all, the hierarchical catalyst allowed one to obtain the oil product with slightly decreased density but 6 times lower viscosity at 25 °C compared to those of the initial feed (Table 2), which is associated with partial cracking and removal of asphaltenes and other resin-like large molecules.

Viscosity, density and fractional composition of the “averaged” mixed oil products obtained over the mesoporous catalyst were not studied since the activity of this sample drastically decreased after ~400 h of hydroprocessing (Fig. 3), which means that the properties of the product must be close to those of the initial feed.

### 3.3 Properties of the Spent Catalysts

According to the differential thermal analysis (DTA) and thermogravimetric analysis (TG), both spent catalysts after 800 h on stream had a significant amount of coke (37–45 wt%), which could be divided into two types: more “loose” coke burning out at 470 °C and more “dense” coke requiring the calcination temperature higher than 580 °C for complete removal (Fig. 4). Generally, a fraction of the “dense” coke increases with time on stream [5] that is consistent with the data obtained in this work. Despite the higher specific surface area and presumably higher initial cracking activity, the mesoporous sample had a slightly lower amount of coke probably because its surface was less accessible for high-molecular reagents due to diffusion restrictions and pore blocking.

The  $N_2/77$  K data indicated that the mesoporous catalyst underwent substantial blocking of the mesopores in the range of 20–40 nm, while the mesopores at 10–20 nm remained relatively intact. It means that the larger mesopores were involved in catalytic transformations to a higher extent

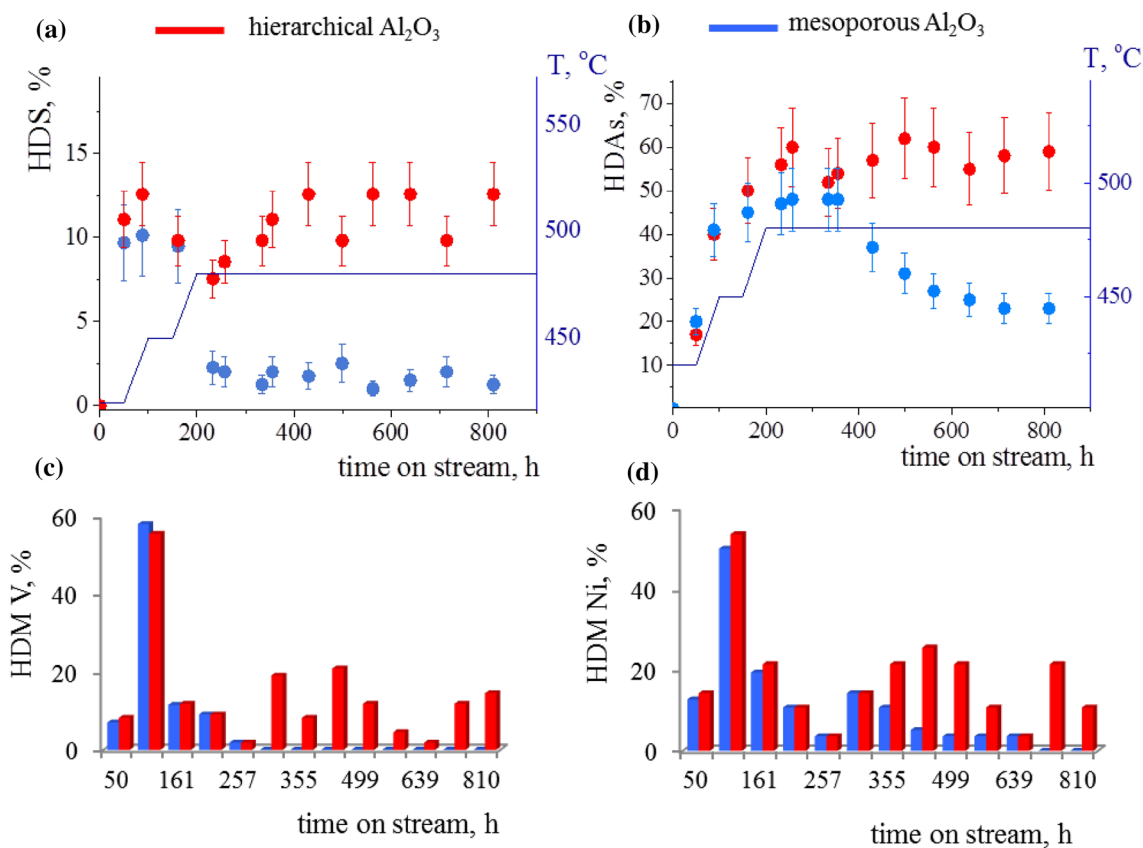


**Fig. 3** Evolution of catalytic activity of the hierarchical and mesoporous catalysts during 800 h on stream: HDS (a), HDAs (b), HDM V (c) and HDM Ni (d) (420 °C, 7 MPa, feed/H<sub>2</sub> 1000, LHSV 1 h<sup>-1</sup>)

**Table 2** Characteristics of heavy feed and oil product after hydroprocessing over the hierarchical catalyst

Parameter	Feed	Product
S, wt%	4.3	3.8
V, ppm	200	148
Ni, ppm	60	41
Viscosity (25 °C), sSt	3710	610
Density, g/cm <sup>3</sup>	0.960	0.956
Gasoline (0–180 °C), wt%	1.9	2.5
Diesel (180–360 °C), wt%	21.5	26.6
Atm. gasoil (360–550 °C), wt%	33.4	35.0
Vacuum gasoil (550–720 °C), wt%	14.8	13.9
Residue (> 720 °C), wt%	28.4	22.0
Asphaltenes, wt%	6.4	2.8

that resulted in pore plugging, which, in turn, was intensive due to the quite small pore mouths and poor transport of the reaction products from the pellet. The hierarchical sample, on the contrary, was shown to acquire additional pores in the range 10–40 nm, which must be ascribed to the formation of coke species on the surface of macro- and mesopores,

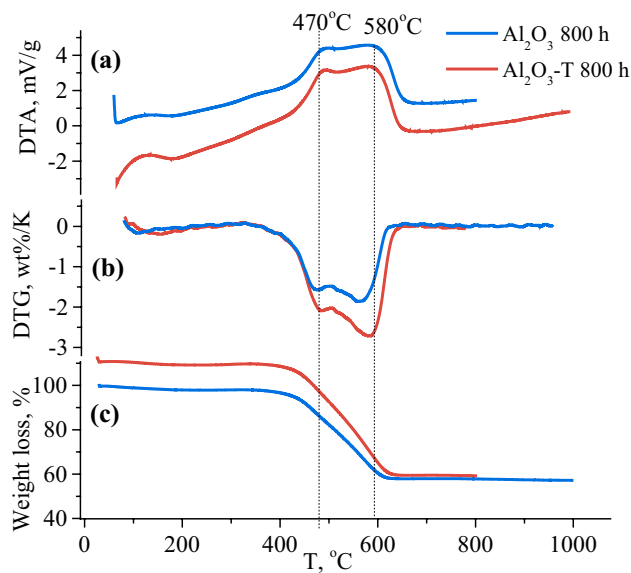


**Fig. 4** DTA (a), differential TG (b) and TG (c) analysis of the fresh and spent catalysts

contributing to the  $S_{\text{BET}}$  and  $V_{\text{N}_2}$ . In this case coke deposits did not cause substantial mesopore blocking due to the wider transport channels.

The Hg porosimetry data also confirmed the notable mesopore plugging by 55% in case of the purely mesoporous catalyst and mesopore narrowing from 15 to 10 nm for the hierarchical sample. The volume of macropores (represented in the curves by the macropore mouths at 40 nm) showed a slight decrease apparently due to the blocking of some mesoporous canals that made those macropores isolated. Nevertheless, taking into account rather long duration of the experiment, macropore blocking does not seem to be intensive and fast under hydroprocessing conditions. The shape of macropores preserved after hydroprocessing which is proved by SEM examination of the spent catalysts (Fig. 2S Supplementary Materials).

### 3.4 Summary

Therefore, given the identical phase composition and similar acidic properties of the catalysts, it is reasonable to conclude that the mesoporous and hierarchical “guard-type” catalysts showed different deactivation behavior only due to the different texture properties. The mesoporous catalyst (pores of 15–26 nm by  $\text{N}_2/77\text{ K}$  and 10–15 nm by Hg porosimetry) experienced strong deactivation after 200–400 h on stream in terms of HDS, HDAs and HDM activity because the mesopores of this size were subjected to substantial blocking by coke deposits under the hydroprocessing conditions. The hierarchical catalyst showed only a 30% decrease in the mesopore volume (vs 55% for the mesoporous sample) and a slight decline in the macropore volume that had no effect on its performance in HDS and HDAs even after 800 h on stream. HDM activity, which usually correlates with the concentration of available adsorption sites, was also shown to be higher for the hierarchical catalyst probably due to better diffusion rates and higher specific surface area accessible for large V or Ni porphyrine-like complexes. The hierarchical texture seems not only to provide wide macro- and mesopores less prone to plugging by coke species but to ensure effective transport of the reaction products out of the small pores preventing them from blockage.

## 4 Conclusion

Two “guard-type” alumina catalysts with mesoporous and hierarchical texture were prepared by the “hard” template method using 250 nm polymer microspheres. According to Hg porosimetry, the mesoporous sample possessed only 10–15 nm mesopores ( $V_{\text{Hg}} = 0.63\text{ cm}^3/\text{cm}^3$ ), while the hierarchical sample had a bimodal pore size distribution with maximum at 15 nm ( $V_{\text{Hg}}(15\text{ nm}) = 0.40\text{ cm}^3/\text{cm}^3$ ) and 40 nm

(mouth of 200 nm macropores,  $V_{\text{Hg}}(40\text{ nm}) = 0.33\text{ cm}^3/\text{cm}^3$ ).

The samples were studied in long-term experiments on hydroprocessing of heavy oil under conditions close to industrial ones. The mesoporous sample underwent the rapid deactivation in HDS and HDM (V) after 200 h on stream, and the remarkable decrease in HDAs and HDM (Ni) after 300–400 h on stream due to the intensive mesopore plugging by 55%.

The hierarchical catalyst did not show any decline in HDS and HDAs during the 800 h experiment, while its HDM activity was reduced due to the poisoning of surface adsorption sites by coke deposits, though to a lesser extent in comparison with the mesoporous analogue. In this case the intrinsic mesopores of alumina showed narrowing down to 10 nm but did not experience such substantial blocking (by 30%) as was observed for the mesoporous catalyst. Apparently, the hierarchical texture seems not only to provide wide macro- and mesopores less prone to plugging by coke species but to ensure effective transport of reaction products out of the small pores preventing them from blockage.

**Acknowledgements** The work was carried out within the framework of the budget project AAAA-A17-117041710077-4 for Boreskov Institute of Catalysis. The authors would like to thank S. V. Cherepanova, N. A. Rudina, T. Ya. Efimenko, V. A., L. N. Atamanova, N. N. Malyarchuk, Trunova, G. S. Lytvak for the characterization of the catalysts and Yu. V. Larichev, P. P. Dik, D. D. Uvarkina and D. O. Novikov for their help with the characterization of the feed and oil products.

## Compliance with Ethical Standards

**Conflict of interest** There are no conflicts to declare.

## References

1. Organization of the Petroleum Exporting Countries (2017) Annual statistical bulletin. Organization of the Petroleum Exporting Countries, Vienna
2. Ancheyta J, Alvarez-Majmutov A, Leyva C (2016) Hydrotreating of oil fractions. Multiphase catalytic reactors. Wiley, New York. pp 295–329
3. Castañeda LC, Muñoz JD, Ancheyta J (2014) Current situation of emerging technologies for upgrading of heavy oils. *Catal Today* 220–222:248–273. <https://doi.org/10.1016/j.cattod.2013.05.016>
4. Ancheyta J, Speight JG (2007) Hydroprocessing of heavy oils and residua. CRC Press, Boca Raton
5. Ancheyta J (2016) Deactivation of hydroprocessing catalysts. Deactivation of heavy oil hydroprocessing catalysts: fundamentals and modeling. Wiley, New York. pp 89–126
6. Baltus RE, Anderson JL (1983) Hindered diffusion of asphaltenes through microporous membranes. *Chem Eng Sci* 38:1959–1969
7. Chiang C-L, Tiou H-H (1992) Optimal design for the residual oil hydrodemetallation in a fixed bed reactor. *Chem Eng Comm* 117:383–399
8. Ruckenstein E, Tsai HC (1981) Optimum pore size for the catalytic conversion of large molecules. *AIChE J* 27:697–699

9. Shimura M, Shiroto Y, Takeuchi C (1986) Effect of Catalyst pore structure on hydrotreating of heavy oil. *Ind Eng Chem Fundam* 25:330–337. <https://doi.org/10.1021/i100023a005>
10. Leyva C, Ancheyta J, Marley L et al (2014) Characterization study of NiMo/SiO<sub>2</sub>-Al<sub>2</sub>O<sub>3</sub> spent hydroprocessing catalysts for heavy oils. *Catal Today* 220–222:89–96. <https://doi.org/10.1016/j.catto.2013.10.007>
11. Liu ZY, Chen SL, Dong P, Ge XJ (2012) Diffusion of heavy oil in SiO<sub>2</sub> model catalyst and FCC catalyst. *Adv Mater Res* 550–553:158–163. <https://doi.org/10.4028/www.scientific.net/AMR.550-553.158>
12. Guichard B, Gaulier F, Barbier J et al (2018) Asphaltenes diffusion/adsorption through catalyst alumina supports—influence on catalytic activity. *Catal Today* 305:49–57. <https://doi.org/10.1016/j.cattod.2017.10.016>
13. Rao SM, Coppens MO (2012) Increasing robustness against deactivation of nanoporous catalysts by introducing an optimized hierarchical pore network-application to hydrodemetalation. *Chem Eng Sci* 83:66–76
14. Dong Y, Xu Y, Zhang Y et al (2018) Synthesis of hierarchically structured alumina support with adjustable nanocrystalline aggregation towards efficient hydrodesulfurization. *Appl Catal A Gen* 559:30–39. <https://doi.org/10.1016/j.apcata.2018.04.007>
15. Dong Y, Chen Z, Xu Y et al (2017) Template-free synthesis of hierarchical meso-macroporous  $\Gamma$ -Al<sub>2</sub>O<sub>3</sub> support: superior hydrodemetalization performance. *Fuel Process Technol* 168:65–73. <https://doi.org/10.1016/j.fuproc.2017.08.034>
16. Absi-Halabi M, Stanislaus A, Al-Mughni T et al (1995) Hydroprocessing of vacuum residues: relation between catalyst activity, deactivation and pore size distribution. *Fuel* 74:1211–1215. [https://doi.org/10.1016/0016-2361\(94\)00042-P](https://doi.org/10.1016/0016-2361(94)00042-P)
17. Sane RC, Tsotsis TT, Webster IA, Ravi-Kumar VS (1992) Studies of asphaltene diffusion and structure and their implications for resid upgrading. *Chem Eng Sci* 47:2683–2688
18. Wang WP, Guin JA (1991) A comparison of unimodal and bimodal catalyst deactivation behavior in a model compound system with rapid coke deposition. *Fuel Process Technol* 28:149–166. [https://doi.org/10.1016/0378-3820\(91\)90046-F](https://doi.org/10.1016/0378-3820(91)90046-F)
19. Khaleel A, Al-Mansouri S (2010) Meso-macroporous  $\gamma$ -alumina by template-free sol-gel synthesis: The effect of the solvent and acid catalyst on the microstructure and textural properties. *Colloids Surfaces A Physicochem Eng Asp* 369:272–280. <https://doi.org/10.1016/j.colsurfa.2010.08.040>
20. Yabuki M, Takahashi R, Sato S et al (2002) Silica–alumina catalysts prepared in sol–gel process of TEOS with organic additives. *Phys Chem Chem Phys* 4:4830–4837. <https://doi.org/10.1039/b205645c>
21. Stanislaus A, Al-Dolama K, Absi-Halabi M (2002) Preparation of a large pore alumina-based HDM catalyst by hydrothermal treatment and studies on pore enlargement mechanism. *J Mol Catal A Chem* 181:33–39. [https://doi.org/10.1016/S1381-1169\(01\)00353-3](https://doi.org/10.1016/S1381-1169(01)00353-3)
22. Li Y, Peng C, Li L, Rao P (2014) Self-assembled 3D hierarchically structured gamma alumina by hydrothermal method. *J Am Ceram Soc* 97:35–39. <https://doi.org/10.1111/jace.12652>
23. Dong Y, Yu X, Zhou Y et al (2018) Towards active mesoporous hydrotreating catalysts: synthesis and assembly of mesoporous alumina microspheres. *Catal Sci Technol* 8:1892–1904. <https://doi.org/10.1039/c7cy02621h>
24. Dupin T, Lavina J, Poisson R (1993) Process for the preparation of alumina agglomerates. United States patent US
25. Mendoza-Nieto JA, Vera-Vallejo O, Escobar-Alarcón L et al (2013) Development of new trimetallic NiMoW catalysts supported on SBA-15 for deep hydrodesulfurization. *Fuel* 110:268–277. <https://doi.org/10.1016/j.fuel.2012.07.057>
26. Boahene PE, Soni KK, Dalai AK, Adjaye J (2011) Application of different pore diameter SBA-15 supports for heavy gas oil hydrotreatment using FeW catalyst. *Appl Catal A Gen* 402:31–40. <https://doi.org/10.1016/j.apcata.2011.05.005>
27. Ruud Snel (1988) Control of the porous structure of amorphous silica–alumina: V. The effect of compaction. *Appl Catal* 36:249–258
28. Trimm DL, Stanislaus A (1986) The control of pore size in alumina catalyst supports: a review. *Appl Catal* 21:215–238. [https://doi.org/10.1016/S0166-9834\(00\)81356-1](https://doi.org/10.1016/S0166-9834(00)81356-1)
29. López-Salinas E, E JG, Hernández-Cortez JG et al (2005) Long-term evaluation of NiMo/alumina–carbon black composite catalysts in hydroconversion of Mexican 538 °C + vacuum residue. *Catal Today* 109:69–75
30. Chen S-L, Dong P, Xu K et al (2007) Large pore heavy oil processing catalysts prepared using colloidal particles as templates. *Catal Today* 125:143–148
31. Su B-L, Sanchez C, Yang X-Y (2012) Hierarchically structured porous materials: from nanoscience to catalysis, separation, optics, energy, and life science. Wiley, New York
32. Li H, Sheng-Li C, Peng D (2009) Preparation, characterization and catalytic performance of novel macroporous catalysts for heavy oil hydrogenation. *Ranliao Huaxue Xuebao* 37:444–447
33. Zi L, Sheng C, Peng D (2012) Novel macroporous residua FCC catalysts. *Fuel Chem Technol* 40
34. Nguyen-Huy C, Shin EW (2016) Hierarchical macro-mesoporous Al<sub>2</sub>O<sub>3</sub>-supported NiK catalyst for steam catalytic cracking of vacuum residue. *Fuel* 169:1–6. <https://doi.org/10.1016/j.fuel.2015.11.088>
35. Liu Z, Dong P (2012) Preparation of macroporous catalysts and their performance in catalytic cracking of heavy oil. *J Fuel Chem Technol* 40:1092–1097
36. Han D, Li X, Zhang L et al (2012) Hierarchically ordered meso/macroporous  $\gamma$ -alumina for enhanced hydrodesulfurization performance. *Microporous Mesoporous Mater* 158:1–6. <https://doi.org/10.1016/j.micromeso.2012.03.022>
37. Semeykina VS, Malkovich EG, Bazaikin YV et al (2018) Optimal catalyst texture in macromolecule conversion: a computational and experimental study. *Chem Eng Sci* 188:1–10. <https://doi.org/10.1016/j.ces.2018.05.005>
38. Larichev YV, Martyanov ON (2018) The dynamics of asphaltene aggregates in heavy crude oils on a nanometer scale studied via small-angle X-ray scattering in situ. *J Pet Sci Eng* 165:575–580
39. Parkhomchuk EV, Semeykina VS, Sashkina KA et al (2016) Synthesis of polystyrene beads for hard-templating of three-dimensionally ordered macroporosity and hierarchical texture of adsorbents and catalysts. *Top Catal*. <https://doi.org/10.1007/s11244-016-0719-3>
40. Semeykina V, Parkhomchuk E, Polukhin A et al (2015) CoMoNi catalyst texture and surface properties in heavy oil processing. Part I: hierarchical macro/mesoporous alumina support. *Ind Eng Chem Res* 55:3535–3545. <https://doi.org/10.1021/acs.iecr.5b04730>
41. Yumoto M, Kukes SG, Klein MT, Gates BC (1996) Catalytic Hydroprocessing of Aromatic Compounds: Effects of Nickel and Vanadium Sulfide Deposits on Reactivities and Reaction Networks. *Ind Eng Chem Res* 35:3203–3209. <https://doi.org/10.1021/ie960023f>
42. Hubaut R (2007) Vanadium-based sulfides as hydrotreating catalysts. *Appl Catal A Gen* 322:121–128. <https://doi.org/10.1016/j.apcata.2007.01.020>

**Publisher's Note** Springer Nature remains neutral with regard to jurisdictional claims in published maps and institutional affiliations.



## Affiliations

**Viktoriya S. Semeykina<sup>1</sup> · Alexander V. Polukhin<sup>1</sup> · Anton I. Lysikov<sup>1</sup> · Andrey V. Kleymenov<sup>2</sup> · Konstantin V. Fedotov<sup>2</sup> · Ekaterina V. Parkhomchuk<sup>1</sup>**

<sup>1</sup> Boreskov Institute of Catalysis SB RAS, pr. Lavrentieva 5, Novosibirsk, Russia

<sup>2</sup> Gazprom Neft, Pochtamskaya st. 3-5, St. Petersburg, Russia